

# Cytochrome $b_{562}$ folding triggered by electron transfer: Approaching the speed limit for formation of a four-helix-bundle protein

(protein folding/guanidine hydrochloride/contact order)

PERNILLA WITTUNG-STAFSHED<sup>\*</sup>, JENNIFER C. LEE, JAY R. WINKLER<sup>†</sup>, AND HARRY B. GRAY<sup>†</sup>

Beckman Institute, California Institute of Technology, Pasadena, CA 91125

Contributed by Harry B. Gray, April 6, 1999

**ABSTRACT** Ferrocycytochrome  $b_{562}$  [Fe(II)cyt  $b_{562}$ ] folding can be triggered by photoinduced electron transfer to unfolded Fe(III)cyt  $b_{562}$  in 2–3 M guanidine hydrochloride solutions. The folding rates increase with decreasing guanidine hydrochloride; the extrapolated time constant for this folding process in the absence of denaturant (5  $\mu$ s) is near the predicted value for intrachain diffusion. The relatively smooth energy landscape indicated for Fe(II)cyt  $b_{562}$  folding accords with the helical, highly symmetrical structure of the protein.

Spontaneous refolding of proteins occurs on timescales that range from microseconds to hours (1–10). Cytochrome  $b_{562}$  (cyt  $b_{562}$ ), a soluble 106-residue heme protein from *Escherichia coli* (11–14), folds relatively rapidly (9, 15). The protein is comprised of four antiparallel  $\alpha$ -helices that wrap into a left-handed bundle; the heme is inserted among the helices, axially ligated by Met7 and His102 (Fig. 1) (16). The heme reduction potential in the folded state [189 mV vs. normal hydrogen electrode (pH 7) (17)] is  $\approx$ 330 mV higher than in the unfolded form [–150 mV (18, 19)], indicating that the driving force for folding is greater for the reduced than for the oxidized protein (9, 15, 20, 21). Guanidine hydrochloride (GuHCl) reversibly unfolds the oxidized protein with a midpoint at 1.8 M (pH 7). Unfolding the reduced protein requires a GuHCl concentration  $>$ 5 M and, owing to heme dissociation, is irreversible. Under suitable denaturing conditions (2 M  $\leq$  [GuHCl]  $\leq$  3 M), electron transfer to unfolded Fe(III)cyt  $b_{562}$  initiates folding of the reduced protein. Earlier, it was reported that the native low-spin Fe(II) protein forms  $\approx$ 1 ms after photochemical electron transfer to unfolded Fe(III)cyt  $b_{562}$  (15).

We have investigated the dependence of the Fe(II)cyt  $b_{562}$  folding kinetics on GuHCl concentration. Extrapolation of the observed rate constants to zero denaturant concentration suggests that the folding of this four-helix-bundle in water approaches the theoretical speed limit for intrachain diffusion of the polypeptide.

## MATERIALS AND METHODS

Guanidine hydrochloride (Sigma, ultrapure grade), tris(2,2'-bipyridine)ruthenium(II) chloride (Strem, Newburyport, MA), and 1,4-dihydropyridinyladenine dinucleotide (NADH, Sigma) were used as received. *Para*-methoxydimethylaniline (*p*MDMA) was synthesized according to a published procedure (22).

Plasmid (pNS207), containing the cytochrome  $b_{562}$  gene (provided by S. G. Sligar, University of Illinois), was expressed in *E. coli* (strain BL21). Cyt  $b_{562}$  was isolated and purified according to a procedure given by Farrow (23). The purity of

proteins used in all experiments was assessed from the 418:280 nm absorbance ( $A_{418}/A_{280} = 5.6$ –6.0). Protein concentrations were determined by using the extinction coefficients  $\epsilon_{418} = 0.117 \mu\text{M}^{-1}\text{cm}^{-1}$  [Fe(III)] and  $\epsilon_{426} = 0.180 \mu\text{M}^{-1}\text{cm}^{-1}$  [Fe(II)] (12, 24). Unfolding curves for Fe(III)- and Fe(II)cyt  $b_{562}$  were generated from absorption and far-UV circular dichroism spectra according to standard procedures (25). In experiments with the Fe(II) protein, a slight excess of sodium dithionite was added to keep the unfolded protein in the reduced state. GuHCl stock solutions were adjusted to pH 7.0–7.1 by using 1.0 M NaOH. The concentration of GuHCl was determined through measurements of the solution refractive index (Milton Roy Abbe-3L Refractometer) (25).

Steady-state absorption spectra were measured on a Hewlett-Packard 8452 diode array spectrophotometer. Circular dichroism spectra were obtained by using an Aviv 62ADS spectropolarimeter (Aviv Associates, Lakewood, NJ). Transient absorption kinetics measurements were made as described (26). The excitation source was a XeCl excimer-pumped dye laser (480 nm, 25 ns, 1–4 mJ) in experiments with Ru(bpy) $_3^{2+}$  and the third harmonic (355 nm) of a Q-switched Nd:YAG laser in experiments using NADH as the photoreductant. Samples for folding kinetics measurements were held in 1-mm sealed cuvettes (0.8–1.5 ml) and contained the following: cyt  $b_{562}$  (15–100  $\mu$ M); either Ru(bpy) $_3^{2+}$  (1.0–1.5 equivalent) and *p*MDMA ( $\approx$ 10 mM) or NADH (2.0–2.5 equivalent); and GuHCl (2–3 M, pH 6.6). Samples were deoxygenated by repeated evacuation/Ar-fill cycles on a Schlenk line. At each GuHCl concentration, the reported rate constant is an average of several kinetics traces.

The yield of folded reduced protein ( $\Phi_f$ ), relative to unfolded reduced protein generated by laser excitation, was calculated from initial and final absorption changes at each GuHCl concentration. The extinction coefficient for the unfolded reduced protein was determined by using a reductive flash quench procedure. Laser-excited Ru(bpy) $_3^{2+}$  was quenched with *p*MDMA to generate Ru(bpy) $_3^{3+}$  and *p*MDMA $^{\cdot+}$ . The concentrations of the charge separated products were determined from their molar difference spectra. The photochemically generated Ru(bpy) $_3^{3+}$  reduces unfolded Fe(III)cyt  $b_{562}$  in  $<$ 10  $\mu$ s. On complete reduction of the heme, the transient spectrum contains contributions from *p*MDMA $^{\cdot+}$  and unfolded Fe(II)cyt  $b_{562}$  at known concentrations. Extinction coefficients for unfolded Fe(II)cyt  $b_{562}$  then were determined from the transient kinetics at various wavelengths by subtracting the contribution from *p*MDMA $^{\cdot+}$ .

The observed rate constant ( $k_{\text{obsd}}$ ) was interpreted as the sum of a folding rate constant ( $k_f$ ) and a dissociation rate constant ( $k_{\text{diss}}$ ):

Abbreviations: ACBP, acyl CoA binding protein; bpy, 2,2'-bipyridine; cyt  $b_{562}$ , cytochrome  $b_{562}$ ; GuHCl, guanidine hydrochloride; *p*MDMA, *para*-methoxydimethylaniline.

<sup>\*</sup>Present Address: Chemistry Department, Tulane University, New Orleans, LA 70118.

<sup>†</sup>To whom reprint requests should be addressed. e-mail: hgcm@its.caltech.edu.

The publication costs of this article were defrayed in part by page charge payment. This article must therefore be hereby marked "advertisement" in accordance with 18 U.S.C. §1734 solely to indicate this fact.

PNAS is available online at www.pnas.org.

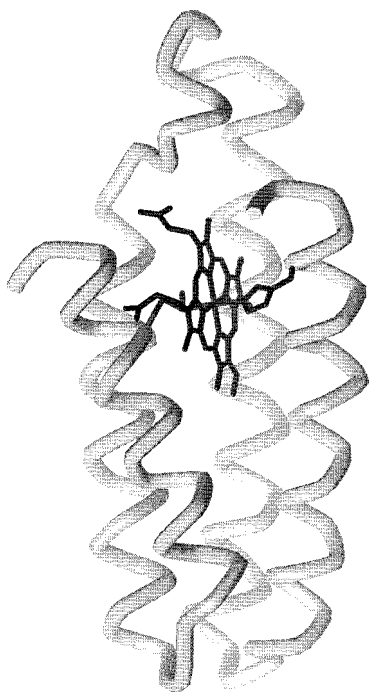


FIG. 1. Cyt  $b_{562}$  structure (Brookhaven Protein Data Bank, accession no. 256B). The heme is coordinated by two axial ligands, Met 7 and His 102. The cytochrome  $b_{562}$  bundle is in an up-down-up-down arrangement, with the four helices almost perfectly parallel to each other.

$$k_{\text{obsd}} = k_f + k_{\text{diss}}$$

$$k_f = k_{\text{obsd}}\Phi_f$$

Folding rate constants were extracted from observed rates by using the spectroscopically determined folding yields.

## RESULTS

The absorption spectra of the oxidized and reduced states of folded cyt  $b_{562}$  show Soret-region features that are characteristic of low-spin  $d^5$  and  $d^6$  hemes (19). On GuHCl denaturation of Fe(III)cyt  $b_{562}$ , the Soret absorption blue-shifts, broadens, and loses intensity at the maximum; these changes in the spectrum reflect the formation of a high-spin  $d^5$  heme (Fig. 2). GuHCl titrations probed by changes in absorbance or circular dichroism spectra indicate that the unfolding midpoint for Fe(III)cyt  $b_{562}$  (1.8 M) is much lower than that for reduced protein (5.7 M) (Fig. 3). The unfolded oxidized protein spontaneously refolds on dilution of GuHCl, confirming that the heme stays bound to the polypeptide for protein concentrations  $>10 \mu\text{M}$  (27). Unfolded Fe(II)cyt  $b_{562}$ , however, does not readily refold on dilution of the denaturant; heme dissociation is likely responsible for this behavior. Between 2 and 3 M GuHCl (pH 7), a significant amount of folded Fe(II)cyt  $b_{562}$  is observed on addition of sodium dithionite to solutions of unfolded Fe(III)cyt  $b_{562}$  (2.33 M GuHCl, 50% yield; 3.02 M, 30%). At higher GuHCl concentrations, heme dissociation from the peptide appears to be faster than protein folding. Measurements of Fe(II)cyt  $b_{562}$  kinetics were, therefore, confined to the 2–3 M GuHCl concentration range.

The folding of Fe(II)cyt  $b_{562}$  was initiated by laser excitation (355 nm) of NADH to produce two powerful reductants, a solvated electron and the  $\text{NAD}^\bullet$  radical (15, 28, 29). The initial transient spectrum ( $<100 \mu\text{s}$ ) reflects formation of reduced unfolded protein. The transient spectrum recorded 10 ms after

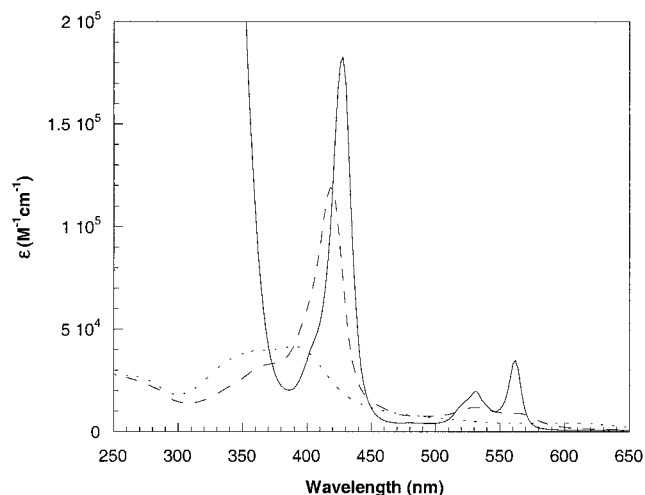


FIG. 2. Soret absorption of folded Fe(III) (dashed line), folded Fe(II) (solid line), and unfolded Fe(III) (dotted line) cyt  $b_{562}$ .

excitation (2.5 M GuHCl) agrees well with steady-state absorption differences between unfolded Fe(III)cyt  $b_{562}$  and folded Fe(II)cyt  $b_{562}$  (15), indicating that folding has occurred on this timescale. Kinetics were monitored by Soret absorption changes (400–430 nm) that indicate the formation of a low-spin ferroheme. The folding reactions were slower at higher GuHCl concentrations; the observed first-order rate constants ( $k_{\text{obsd}}$ ) range from  $3.3(7) \times 10^3$  to  $7.4(9) \times 10^3 \text{ s}^{-1}$  (2–3 M GuHCl). Specific rate constants for formation of low-spin folded cyt  $b_{562}$ , extracted from the observed rate constants, vary from  $1.5(2) \times 10^3$  (2.2 M GuHCl) to  $3.0(9) \times 10^2 \text{ s}^{-1}$  (3.0 M GuHCl) (Fig. 4). (The rate constants for the competing heme-dissociation process range from 3 to  $7 \times 10^3 \text{ s}^{-1}$  between 2 and 3 M GuHCl.) Although a relatively narrow range of GuHCl concentrations was explored, there appears to be a linear relationship between the logarithm of the folding rate and the GuHCl concentration (Fig. 4). Extrapolation to 0 M GuHCl suggests a time constant of  $\approx 5 \mu\text{s}$  for folding Fe(II)cyt  $b_{562}$  in water.<sup>‡</sup>

## DISCUSSION

A recent molecular-dynamics simulation carried out on an unfolded 36-residue protein suggests that partly folded struc-

<sup>‡</sup>Note that the highest measured rate is  $1.5 \times 10^3 \text{ s}^{-1}$  (at 2.2 M GuHCl).

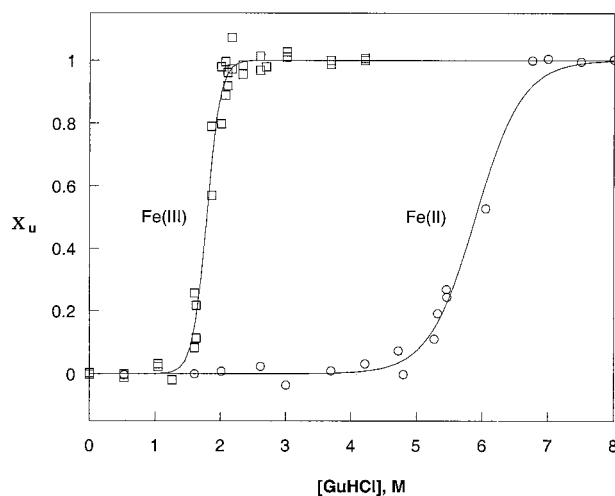


FIG. 3. Denaturant-induced unfolding of Fe(III) and Fe(II) cytochrome  $b_{562}$ , pH 7.

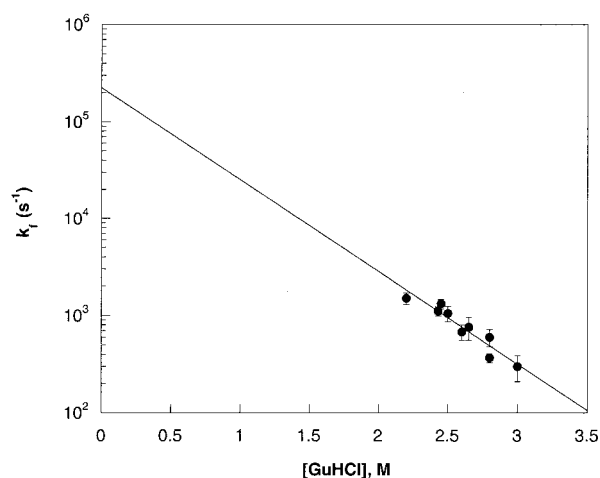


FIG. 4. Variation of ferrocycytochrome  $b_{562}$  folding rates with GuHCl concentration (pH 6.6). Observed rate constants, folding rate constants ([GuHCl], yield of folded protein):  $3.3(7) \times 10^3$ ,  $1.5(2) \times 10^3$   $s^{-1}$  (2.20 M, 45%);  $3.4(1) \times 10^3$ ,  $1.1(1) \times 10^3$   $s^{-1}$  (2.43 M, 34%);  $6.0(7) \times 10^3$ ,  $1.3(2) \times 10^3$   $s^{-1}$  (2.45 M, 22%);  $3.2(6) \times 10^3$ ,  $1.1(2) \times 10^3$   $s^{-1}$  (2.50 M, 33%);  $5.4(2) \times 10^3$ ,  $6.8(2) \times 10^2$   $s^{-1}$  (2.60 M, 13%);  $9.5(3) \times 10^3$ ,  $7.6(2) \times 10^2$   $s^{-1}$  (2.65 M, 8%);  $5.5(6) \times 10^3$ ,  $6.0(1) \times 10^2$   $s^{-1}$  (2.80 M, 6%);  $6.3(2) \times 10^3$ ,  $3.7(4) \times 10^2$   $s^{-1}$  (2.80 M, 9%);  $7.4(9) \times 10^3$ ,  $3.0(9) \times 10^2$   $s^{-1}$  (3.00 M, 4%).

tures can occur within tens of nanoseconds (30). Experimental studies on apomyoglobin (134 residues) indicate that some secondary structure forms in the first 10  $\mu s$  of folding (31, 32). Polymer diffusion models have been used to estimate that the minimum time constant for folding a small, single-domain protein to its native structure is on the order of 1  $\mu s$  (8, 33). More recent estimates suggest a lower limit of 0.2  $\mu s$  for protein folding (34). Our extrapolated folding time for Fe(I-*I*)cyt  $b_{562}$  approaches this limit.

Another four-helix bundle, the acyl CoA binding protein (ACBP), folds more slowly than Fe(II)cyt  $b_{562}$  [700  $s^{-1}$ , 20°C (35, 36)]. ACBP has a so-called up-down-down-up four-helix bundle structure held together by hydrophobic junctions, where the helices interact pairwise or in groups of three (37). By contrast, the cyt  $b_{562}$  bundle is an up-down-up-down arrangement, and the four helices are almost perfectly parallel to each other (16). ACBP is less stable than Fe(II) cyt  $b_{562}$  [ $-\Delta G_f = 29$  (35, 36) and  $\approx 43$  kJ/mol (15), respectively], a property that may affect the folding kinetics, because, in general, the tertiary folds of these two proteins are similar. Although reduced horse heart cytochrome *c* is much more stable [ $-\Delta G_f = 74$  kJ/mol (38)] than Fe(II)cyt  $b_{562}$ , it folds much more slowly [estimated folding time of 100  $\mu s$  in aqueous solution (20, 28, 38)]. Part of the difference is undoubtedly attributable to ligand substitution kinetics that retard the folding of cytochrome *c* (28). But even at reduced pH, where the heme in unfolded cytochrome *c* is not misligated, protein folding is still slower than for cyt  $b_{562}$  (5).

Why does folding of Fe(II)cyt  $b_{562}$  occur near the maximum speed limit when the folding of other helical proteins is much slower? Theoretical analysis indicates that symmetrical structures will have relatively smooth energy landscapes for folding (1, 39), and the up-down-up-down four-helix-bundle structure of cytochrome  $b_{562}$  is one of the most symmetrical of protein architectures. It is interesting to note that an inverse correlation between folding rates and contact order (the average relative sequence separation of native contacts) has been observed for a set of single-domain proteins that exhibit two-state folding (40). Although two-state folding has not yet been confirmed in cyt  $b_{562}$ , the contact order of this protein is extremely low, 7.5% (K. W. Plaxco, personal communication), which is consistent with its very local, all helical structure (16).

This low contact order corresponds to a predicted folding time of  $\approx 10$   $\mu s$ , which is in good agreement with our extrapolated value of 5  $\mu s$ . The longer folding times of the helical proteins cytochrome *c* and ACBP (20, 28, 35, 36, 38) are consistent with the predictions of the contact-order model (contact orders: cyt *c*, 11.2%; ACBP, 14%) (40).

The fast folding observed for cyt  $b_{562}$  may be a consequence of the competing heme-dissociation step. Unfolded cyt  $b_{562}$  is expected to be an ensemble of randomly configured, heme-bound polypeptides. The kinetics for conversion of this ensemble into a homogeneous population of folded proteins could be highly heterogeneous. Some configurations in the unfolded ensemble could fold quite rapidly whereas others might require much longer times (41). This division of the unfolded ensemble into fast and slow folding populations can have important implications when a second process competes with folding. In Fe(II)cyt  $b_{562}$ , it is possible that only fast folding is observed because the heme dissociates from the slow-folding configurations. Because the free heme has a relatively weak spectroscopic signature, its presence would be difficult to detect amid a population of folded reduced protein. If heme dissociation does select against slow folding configurations in Fe(II)cyt  $b_{562}$ , then we expect that four-helix bundle *c*-type heme proteins [e.g., cytochrome *c'* (11, 42)] would require much longer times to form fully folded ensembles.

We thank Kevin Plaxco and Peter Wolynes for communication of unpublished results as well as several stimulating discussions. P.W.-S. acknowledges a postdoctoral fellowship from the Swedish Technical Research Council. J.C.L. acknowledges a graduate fellowship from the Ralph M. Parsons Foundation. This work was supported by the National Science Foundation (Grant MCB 9630465).

- Onuchic, J. N., Lutheyschulten, Z. & Wolynes, P. G. (1997) *Annu. Rev. Phys. Chem.* **48**, 545–600.
- Shakhnovich, E. I. (1997) *Curr. Opin. Struct. Biol.* **7**, 29–40.
- Dobson, C. M., Sali, A. & Karplus, M. (1998) *Angew. Chem. Int. Ed. Eng.* **37**, 868–893.
- Dill, K. A. & Chan, H. S. (1997) *Nat. Struct. Biol.* **4**, 10–19.
- Englander, S. W., Sosnick, T. R., Mayne, L. C., Shtilerman, M., Qi, P. X. & Bai, Y. (1998) *Acc. Chem. Res.* **31**, 737–744.
- Shastry, M. C. R., Sauder, J. M. & Roder, H. (1998) *Acc. Chem. Res.* **31**, 717–725.
- Yeh, S.-R., Han, S. & Rousseau, D. L. (1998) *Acc. Chem. Res.* **31**, 727–736.
- Eaton, W. A., Muñoz, V., Thompson, P. A., Henry, E. R. & Hofrichter, J. (1998) *Acc. Chem. Res.* **31**, 745–753.
- Telford, J. R., Wittung-Stafshede, P., Gray, H. B. & Winkler, J. R. (1998) *Acc. Chem. Res.* **31**, 755–763.
- Dodge, R. W. & Scheraga, H. A. (1996) *Biochemistry* **35**, 1548–1559.
- Moore, G. R. & Pettigrew, G. W. (1990) *Cytochromes c: Evolutionary, Structural, and Physicochemical Aspects* (Springer, New York).
- Itagaki, E. & Hager, L. P. (1966) *J. Biol. Chem.* **241**, 3687–3695.
- Itagaki, E., Palmer, G. & Hager, L. P. (1967) *J. Biol. Chem.* **242**, 2272–2277.
- Nikkila, H., Gennis, R. B. & Sligar, S. G. (1991) *Eur. J. Biochem.* **202**, 309–313.
- Wittung-Stafshede, P., Gray, H. B. & Winkler, J. R. (1997) *J. Am. Chem. Soc.* **119**, 9562–9563.
- Hamada, K., Bethge, P. H. & Mathews, F. S. (1995) *J. Mol. Biol.* **247**, 947–962.
- Barker, P. D., Butler, J. L., de Oliveira, P., Hill, H. A. O. & Hunt, N. I. (1996) *Inorg. Chim. Acta* **252**, 71–77.
- Bixler, J., Bakker, G. & McLendon, G. (1992) *J. Am. Chem. Soc.* **114**, 6938–6939.
- Tezcan, F. A., Winkler, J. R. & Gray, H. B. (1998) *J. Am. Chem. Soc.* **120**, 13383–13388.
- Pascher, T., Chesick, J. P., Winkler, J. R. & Gray, H. B. (1996) *Science* **271**, 1558–1560.
- Winkler, J. R., Wittung-Stafshede, P., Leckner, J., Malmström,

- B. G. & Gray, H. B. (1997) *Proc. Natl. Acad. Sci. USA* **94**, 4246–4249.
22. Sekiya, M. & Leonard, N. J. (1968) *J. Org. Chem.* **33**, 318–312.
23. Farrow, N. A. (1999) Ph.D. thesis (California Institute of Technology, Pasadena, CA).
24. Moore, G. R., Williams, R. J. P., Peterson, J., Thomson, A. J. & Mathews, F. S. (1985) *Biochim. Biophys. Acta* **829**, 83–96.
25. Pace, N. C., Shirley, B. A. & Thomson, J. A. (1990) in *Protein Structure: A Practical Approach*, ed. Creighton, T. F. (IRL, Oxford), pp. 311–330.
26. Stowell, M. H. B., Larsen, R. W., Winkler, J. R., Rees, D. C. & Chan, S. I. (1993) *J. Phys. Chem.* **97**, 3054–3057.
27. Robinson, C. R., Liu, Y., Thomson, J. A., Sturtevant, J. M. & Sligar, S. G. (1997) *Biochemistry* **36**, 16141–16146.
28. Telford, J. R., Tezcan, F. A., Gray, H. B. & Winkler, J. R. (1999) *Biochemistry* **38**, 1944–1949.
29. Oriti, Y. (1993) *Biochemistry* **32**, 11910–11914.
30. Duan, Y., Wang, L. & Kollman, P. A. (1998) *Proc. Natl. Acad. Sci. USA* **95**, 9897–9902.
31. Gruebele, M., Sabelko, J., Ballew, R. & Ervin, J. (1998) *Acc. Chem. Res.* **31**, 699–707.
32. Dyer, R. B., Gai, F., Woodruff, W. H., Gilmanshin, R. & Callender, R. H. (1998) *Acc. Chem. Res.* **31**, 709–716.
33. Hagen, S. J., Hofrichter, J., Szabo, A. & Eaton, W. A. (1996) *Proc. Natl. Acad. Sci. USA* **93**, 11615–11617.
34. Thirumalai, D. (1999) *J. Phys. Chem. B* **103**, 608–610.
35. Kragelund, B. B., Robinson, C. V., Knudsen, J., Dobson, C. M. & Poulsen, F. M. (1995) *Biochemistry* **34**, 7217–7224.
36. Kragelund, B. B., Højrup, P., Jensen, M. S., Schjerling, C. K., Juul, E., Knudsen, J. & Poulsen, F. M. (1996) *J. Mol. Biol.* **256**, 187–200.
37. Andersen, K. V. & Poulsen, F. (1992) *J. Mol. Biol.* **226**, 1131–1141.
38. Mines, G. A., Pascher, T., Lee, S. C., Winkler, J. R. & Gray, H. B. (1996) *Chem. Biol.* **3**, 491–497.
39. Wolynes, P. G. (1996) *Proc. Natl. Acad. Sci. USA* **93**, 14249–14255.
40. Plaxco, K. W., Simons, K. T. & Baker, D. (1998) *J. Mol. Biol.* **277**, 985–994.
41. Guo, Z. & Thirumalai, D. (1996) *J. Mol. Biol.* **263**, 323–343.
42. Bertini, I., Dikiy, A., Luchinat, C., Macinai, R. & Viezzoli, M. S. (1998) *Inorg. Chem.* **37**, 4814–4821.